IGF2BP2-dependent STIM1 inhibition protects against LPS-induced pneumonia *in vitro* by alleviating endoplasmic reticulum stress and the inflammatory response

WEI ZHOU[1], QIGANG DAI[2], NING SU[3], ZHIHUI LIU[4] and JINXING HU[5,6]

[1]Department of Pathology, Guangzhou Chest Hospital, Guangzhou, Guangdong 510095; [2]Department of Oncology, The First Affiliated Hospital of Guangdong Pharmaceutical University, Guangzhou, Guangdong 510699; Departments of [3]Oncology, [4]Clinical Laboratory and [5]Tuberculosis, Guangzhou Chest Hospital, Guangzhou, Guangdong 510095; [6]State Key Laboratory of Respiratory Disease, Guangzhou Medical University, Guangzhou, Guangdong 511495, P.R. China

Received May 19, 2023; Accepted August 3, 2023

DOI: 10.3892/etm.2023.12273

Abstract. Pneumonia is a disease caused by inflammation and has high morbidity and mortality rates. Stromal interaction molecule 1 (*STIM1*) is involved in the regulation of inflammatory processes. However, to the best of the authors' knowledge, the role of *STIM1* in pneumonia has not yet been reported. In the present study, lipopolysaccharide (LPS) was administered to A549 cells to construct a cell damage model. The expression of *STIM1* in the model cells was detected by western blotting and reverse transcription-quantitative PCR. Then, *STIM1* expression was inhibited and cell survival was detected by Cell Counting Kit-8 and flow cytometry. The expression of inflammatory factors was detected by enzyme-linked immunosorbent assay and endoplasmic reticulum stress (ERS)-related proteins were detected by immunofluorescence and western blotting. Subsequently, the relationship between insulin-like growth factor 2 mRNA binding protein 2 (IGF2BP2) and *STIM1* was verified by RNA-binding protein immunoprecipitation assay and actinomycin D treatment. Finally, the regulatory mechanism of IGF2BP2 and *STIM1* in LPS-induced A549 cells was further investigated. The results of the present study demonstrated that *STIM1* expression was increased in LPS-induced A549 cells and that *STIM1* knockdown inhibited LPS-induced A549 cell apoptosis and alleviated LPS-induced A549 cell inflammation and ERS. In addition, IGF2BP2 enhanced the stability of *STIM1* mRNA and knockdown of IGF2BP2-regulated *STIM1* expression alleviated LPS-induced ERS and inflammatory responses in A549 cells. In conclusion, knockdown of IGF2BP2-regulated *STIM1* improved cell damage in the LPS-induced pneumonia cell model by alleviating ERS and the inflammatory response.

Correspondence to: Dr Jinxing Hu, Department of Tuberculosis, Guangzhou Chest Hospital, 62 Hengzhigang Road, Yuexiu, Guangzhou, Guangdong 510095, P.R. China
E-mail: hujx830511@163.com

Key words: pneumonia, *STIM1*, *IGF2BP2*, inflammatory response, endoplasmic reticulum stress

Introduction

Pneumonia is a common inflammation-related disease with high morbidity and mortality rates among infectious diseases and is an important health problem worldwide. Persistent inflammatory infection with pneumonia can induce lung tissue damage (1,2). The drugs commonly administered in the clinical treatment of pneumonia include antibiotics and adrenocorticoid hormones (3). However, after treatment with these drugs, the body will develop resistance and significant side effects including gastrointestinal infections and metabolic disturbance (4,5). Therefore, it has become an urgent problem for researchers to improve the treatment efficacy of pneumonia and to understand the underlying mechanism of the disease.

Under pathological conditions, the environment in the endoplasmic reticulum (ER) changes and misfolded and unfolded proteins accumulate in the ER cavity until the ER homeostasis is disrupted. Following this, a series of stress reactions in the ER are triggered to process these misfolded or unfolded proteins and maintain the normal function of cells. This process is called endoplasmic reticulum stress (ERS) (6). Hypoxia, inflammatory response, oxidative stress and other interfering factors can lead to the increase of protein misfolding rate and protein load in the ER, inducing ERS (7). A previous study showed that alleviating inflammation and ERS in pediatric pneumonia can significantly inhibit the development of pediatric pneumonia (8). Therefore, it is beneficial to improve the symptoms of pneumonia by alleviating ERS and inflammation. Previous research has shown that Stromal interaction molecule 1 (*STIM1*)-*Orai1* interaction exacerbates LPS-induced inflammation and ERS in bovine hepatocytes through store-operated calcium entry (9). *STIM1* is a recently discovered vasoactive protein that can participate in the regulation of inflammatory processes (10-13). A previous study has shown that *STIM1* is closely related to activation of the inflammatory response and platelet aggregation after stent implantation in percutaneous coronary intervention (14). In

addition, overexpression of SOX9 can alleviate the inflammatory damage of bronchial epithelial cells induced by cigarette smoke extract by inhibiting *STIM1* (15). Furthermore, silencing *STIM1* expression inactivates NLR pyrin domain containing 3 by promoting the expression of microRNA-223, thereby reducing the inflammatory damage of lung epithelial cells induced by influenza A virus (16). *STIM1* has also been shown to reduce lipopolysaccharide (LPS)-induced inflammation by inhibiting NF-κB signaling in bovine mammary epithelial cells (17). However, there are few studies investigating the regulatory role of *STIM1* on ERS and inflammation in pneumonia.

The present study predicted the potential interaction of the RNA-binding protein insulin-like growth factor 2 mRNA binding protein 2 (*IGF2BP2*) with STIM1 via RBPmap website. *IGF2BP2* belongs to a highly conserved family of RNA-binding proteins whose function is to regulate mRNA localization, stability and translation and fine-tune the physiological function of the encoded protein (18). *IGF2BP2* knockdown inhibited LPS-induced inflammation of lung epithelial cells by targeting caspase 4, thus inhibiting the non-standard scorching pathway (19). So it was hypothesized that *IGF2BP2* can regulate *STIM1* and thus play a role in LPS-induced pneumonia.

In the present study, the role of *STIM1* in an LPS-induced pneumonia cell model and its regulatory mechanism were investigated, to provide a useful theoretical basis for the future clinical treatment of pneumonia.

Materials and methods

Database. The RNA-binding protein IGF2BP2 has a potential interaction with *STIM1*, which was investigated using the web-tool RBPmap (http://rbpmap.technion.ac.il/) that enables prediction of RBP binding on genome sequences from a huge list of experimentally validated motifs of RBPmap database (Table SI) (20).

Cell culture. The human lung adenocarcinoma epithelial cells A549 purchased from the BeNa Culture Collection (cat. no. BNCC337696) and was cultured in Dulbecco's Modified Eagle's Medium (DMEM; Thermo Fisher Scientific, Inc.) containing 10% fetal bovine serum (Gibco; Thermo Fisher Scientific, Inc.) in a 37˚C incubator with 5% carbon dioxide. For the injury model, the cells were placed in 6-well plates ($3x10^5$ cells/well) and incubated for 12 h, before incubation with LPS (10 μg/ml) for a further 24 h (21). LPS induces the human pulmonary epithelial cell line A549 to create a pneumonia model (22,23).

Reverse transcription quantitative PCR (RT-qPCR). The A549 cells in a 6-well plate at a density of $2x10^5$ cells/well were lysed using TRIzol® reagent (Thermo Fisher Scientific, Inc.) and total RNA was purified using a RNeasy Plus Mini Kit (Qiagen, Inc.). Then, cDNA was generated using 1 μg total RNA and a High-Capacity cDNA Reverse Transcription Kit (Applied Biosystems; Thermo Fisher Scientific, Inc.) according to the manufacturer's protocol. The cDNA was then amplified by IQTM SYBR Green Master Mix (Bio-Rad Laboratories, Inc.), which was then quantified using a SYBR-Green detection system (Applied Biosystems; Thermo Fisher Scientific, Inc.). The following thermocycling conditions were used for the qPCR: Initial denaturation at 95˚C for 10 min; 50 cycles of 95˚C for 15 sec and 60˚C for 60 sec. Each reaction was performed three times. Finally, the $2^{-\Delta\Delta Cq}$ quantification method was used to calculate the expression levels of target mRNAs (24). The *GAPDH* mRNA level was used as the normalized standard. The PCR primers were as follows: *STIM1* forward: 5'-GCC TAGGAGGCCCAGGAT-3', reverse: 5'-ACAGCCAAAGGT CAAGTGCT-3'; *IGF2BP2* forward: 5'-GGAACAAGTCA ACACAGACACA-3', reverse: 5'-CGCAGCGGGAAATCA ATCTG-3'; *GAPDH* forward: 5'-AATGGGCAGCCGTTA GGAAA-3', reverse: 5'-GCGCCCAATACGACCAAATC-3'.

Western blotting. The A549 cells were lysed in RIPA buffer and protein contents were determined by the BCA method. In total, 20 μg of proteins was separated by 12% SDS-PAGE and then transferred to PVDF membranes. The membranes blocked with 5% BSA (Sigma-Aldrich; Merck KGaA) for 1 h at room temperature were incubated with primary antibodies STIM1 (1:1,000; cat. no. ab108994; Abcam), Bcl-2 (1:1,000; cat. no. ab182858; Abcam), Bax (1:1,000; cat. no. ab32503; Abcam), glucose-regulated protein 78 (GRP78; 1:1,000; cat. no. ab21685; Abcam), activating transcription factor 6 (ATF6; 1:1,000; cat. no. ab227830; Abcam), C/EBP homologous protein (CHOP) (1:1,000; cat. no. 5554; CST), caspase 12 (1:1,000; cat. no. ab62484; Abcam), PKR-like ER kinase (PERK; 1:1,000; cat. no. ab229912; Abcam), insulin-like growth factor 2 mRNA binding protein 3 (IGF2BP3; 1:1,000; cat. no. ab177477; Abcam), phosphorylated (p-)PERK (1:1,000; cat. no. 3179; CST), GAPDH (1:1,000; cat. no. ab9485; Abcam) overnight at 4˚C. Then, the appropriate horseradish peroxidase-conjugated secondary antibody (1:5,000; cat. no. ab150077; Abcam) was incubated with the membranes for 1 h at 37˚C. GAPDH was used as the internal control. Protein bands were then detected by enhanced chemiluminescence (MilliporeSigma). The western blot images were analyzed using Image J software (V1.8.0, National Institutes of Health).

Cell transfection. Insulin-like growth factor 2 mRNA binding protein 2 (*IGF2BP2*) overexpression lentivirus (Oe-*IGF2BP2*) and the corresponding negative control (Oe-NC; pcDNA3.1) and small interfering (si)RNAs against *STIM1* (si-*STIM1*#1 and si-*STIM1*#2) and their corresponding scrambled sequence negative control (si-NC) were obtained from Shanghai GenePharma Co., Ltd. Transfection was conducted at 37˚C for 48 h using Lipofectamine® 2000 reagent (Invitrogen; Thermo Fisher Scientific, Inc.) according to the manufacturer's protocol. The transfection efficiency was detected by RT-qPCR or western blotting as aforementioned 48 h after transfection. The sequences were as follows: si-*STIM1*#1 sense, 5'-UCAAUUCGGCAA AACUCUGCU-3' and antisense, 5'-CAGAGUUUUGCCGAA UUGACA-3'; si-*STIM1*#2 sense, 5'-UCAGUUUGUGGAUGU UACGGA-3' and antisense, 5'-CGUAACAUCCACAAACUG AUG-3'; si-*IGF2BP2*#1 sense, 5'-AGUAGUUCUCAAACU GAUGCC-3' and antisense, 5'-CAUCAGUUUGAGAACUAC UCC-3'; si-*IGF2BP2*#2 sense, 5'-UCUUGAAGGAGUAGUUCU CAA-3' and antisense, 5'-GAGAACUACUCCUUCAAGAUU-3'; and si-NC sense, 5'-UUCUCCGAACGUGUCACGUTT-3' and antisense, 5'-ACGUGACACGUUCGGAGAATT-3'.

Cell Counting Kit (CCK)-8 assay. A549 cells were seeded into 96-well plates at a density of $5x10^3$ cells/well and were treated accordingly before incubation with 10 μl CCK-8 working solution (MedChemExpress) for 4 h. Absorbance was measured at 450 nm using a microplate reader.

Flow cytometry. A549 cells were seeded into 96-well plates at a density of $2x10^6$ cells/well. After the corresponding incubation, cells were stained with FITC-conjugated annexin V and propidium iodide using an annexin V-FITC apoptosis kit (Beyotime Institute of Biotechnology) for 10 min in the dark at room temperature. Apoptotic cells were quantified by loading the cell mixture onto a CytoFLEX flow cytometry system (Beckman Coulter, Inc.) and FlowJo software (Version 10; FlowJo LLC) was used to analyze the data. Apoptosis rate was calculated as the sum of the early apoptosis rate (the lower right quadrant) and the late apoptosis rate (the upper right quadrant).

Enzyme-linked immunosorbent assay (ELISA). To detect the levels of IL-6 (cat. no. ab178013; Abcam), IL-1β (cat. no. ab214025; Abcam) and TNF-α (cat. no. ab181421; Abcam) in the cell supernatants, related ELISA assay kits were used according to the manufacturer's recommendations.

Immunofluorescence (IF). After treatment, A549 cells were fixed in 4% paraformaldehyde (300 μl/well; Sigma-Aldrich; Merck KGaA), incubated in 0.3% Triton X-100 (500 μl/well; Sigma-Aldrich; Merck KGaA) for 15 min and then blocked with 5% goat serum (Sigma-Aldrich; Merck KGaA). The slides were then stained with CHOP primary antibody (1:300; cat. no. 5554; CST) overnight at 4˚C and the fluorescent secondary antibody (1:500; cat. no. ab150077; Abcam) at 37˚C for 30 min, before being stained with DAPI (MilliporeSigma) for 10 min at room temperature in mounting medium. The cells were observed using an LSM 710 confocal laser microscope system (Carl Zeiss AG).

RNA-binding protein immunoprecipitation (RIP) assay. RIP assays were performed according to the EZ-Magna RIP RNA-binding Protein Immunoprecipitation Kit (MilliporeSigma). The cells were collected and added with 10 ml PBS and 0.01% formaldehyde to crosslink for 15 min. Then 1.4 ml 2 mol/l glycine was added and mixed for 5 min before being centrifuged for 5 min at 1,000 x g at room temperature. After discarding the supernatant, the cells were lysed with RIPA lysis buffer with 20 μl of protein A resin addition and incubated for 1 h at 4˚C. The supernatant was discarded and 50 μl PBS was added for suspension. Total RNA was extracted from suspension with TRIzol® reagent and reverse synthesis of cDNA. Finally, *STIM1* mRNA abundance was detected by RT-qPCR as aforementioned.

RNA stability analysis. After treatment, A549 cells were exposed to 2 μg/ml actinomycin D (Cayman Chemical Company) for 0, 4, 8, 12 or 24 h to block transcription. DMSO (MilliporeSigma) was used as the control reagent. Cell samples were collected at the indicated time points and RNA was extracted. Finally, *STIM1* mRNA expression levels were detected by RT-qPCR as aforementioned (25).

Statistical analysis. The data are presented as the mean ± SD and were analyzed using GraphPad Prism 5 (Dotmatics). The comparisons were assessed using one-way ANOVA followed by Tukey's post hoc test. $P<0.05$ was considered to indicate a statistically significant difference. Each experiment was repeated at least three times.

Results

STIM1 is upregulated in LPS-induced A549 cells and STIM1 knockdown inhibits LPS-induced A549 cell apoptosis. After A549 cells were induced with LPS, the expression of *STIM1* was detected by RT-qPCR and western blotting. The results demonstrated that the expression of *STIM1* was significantly increased after LPS induction, compared with the untreated control cells (Fig. 1A and B). Following this, *STIM1* interference plasmids were constructed, A549 cells were transfected with these plasmids and the transfection efficacy was detected by RT-qPCR and western blotting (Fig. 1C and D). si-*STIM1*#1 was selected for follow-up experiments due to its more prominent interference efficacy. Cells were then divided into the control, LPS, LPS + si-NC and LPS + si-*STIM1* groups. Subsequently, cell viability was measured by CCK-8 and the results demonstrated that cell viability was significantly decreased in the LPS group compared with the control group. Furthermore, compared with the LPS + si-NC group, cell viability was increased in the LPS + si-*STIM1* group (Fig. 1E). Flow cytometry demonstrated that LPS treatment induced cell apoptosis, which was significantly reduced after inhibition of *STIM1* expression (Fig. 1F). Western blotting analysis of apoptosis-related proteins demonstrated that Bcl-2 expression was decreased and Bax expression was increased in the LPS group, compared with the control group. Furthermore, compared with the LPS + si-NC group, Bcl-2 expression was increased and Bax expression was decreased in the LPS + si-*STIM1* group (Fig. 1G).

STIM1 knockdown alleviates LPS-induced inflammation and ERS in A549 cells. ELISA kits were used to detect the levels of inflammatory cytokines and the results indicated that LPS could significantly increase the levels of IL-6, IL-1β and TNF-α. Following inhibition of *STIM1* expression, the levels of the inflammatory cytokines were reversed (Fig. 2A). An IF assay was used to detect the expression of CHOP and it was found that the fluorescence intensity of CHOP was significantly increased after LPS induction, while expression was significantly decreased after *STIM1* inhibition (Fig. 2B). Western blotting analysis demonstrated that GRP78, ATF6, CHOP, caspase 12 and p-PERK expression levels were increased in the LPS group compared with the control group. Furthermore, compared with the LPS + si-NC group, the expression of the aforementioned proteins in the LPS + si-*STIM1* group were decreased (Fig. 2C).

IGF2BP2 enhances the stability of STIM1 mRNA. The results of RT-qPCR and western blotting assays demonstrated that *IGF2BP2* levels were also significantly increased in LPS-induced A549 cells (Fig. 3A and B). The binding ability of IGF2BP2 to *STIM1* mRNA was detected using a RIP assay; as expected, *STIM1* mRNA was enriched in RNA pulled

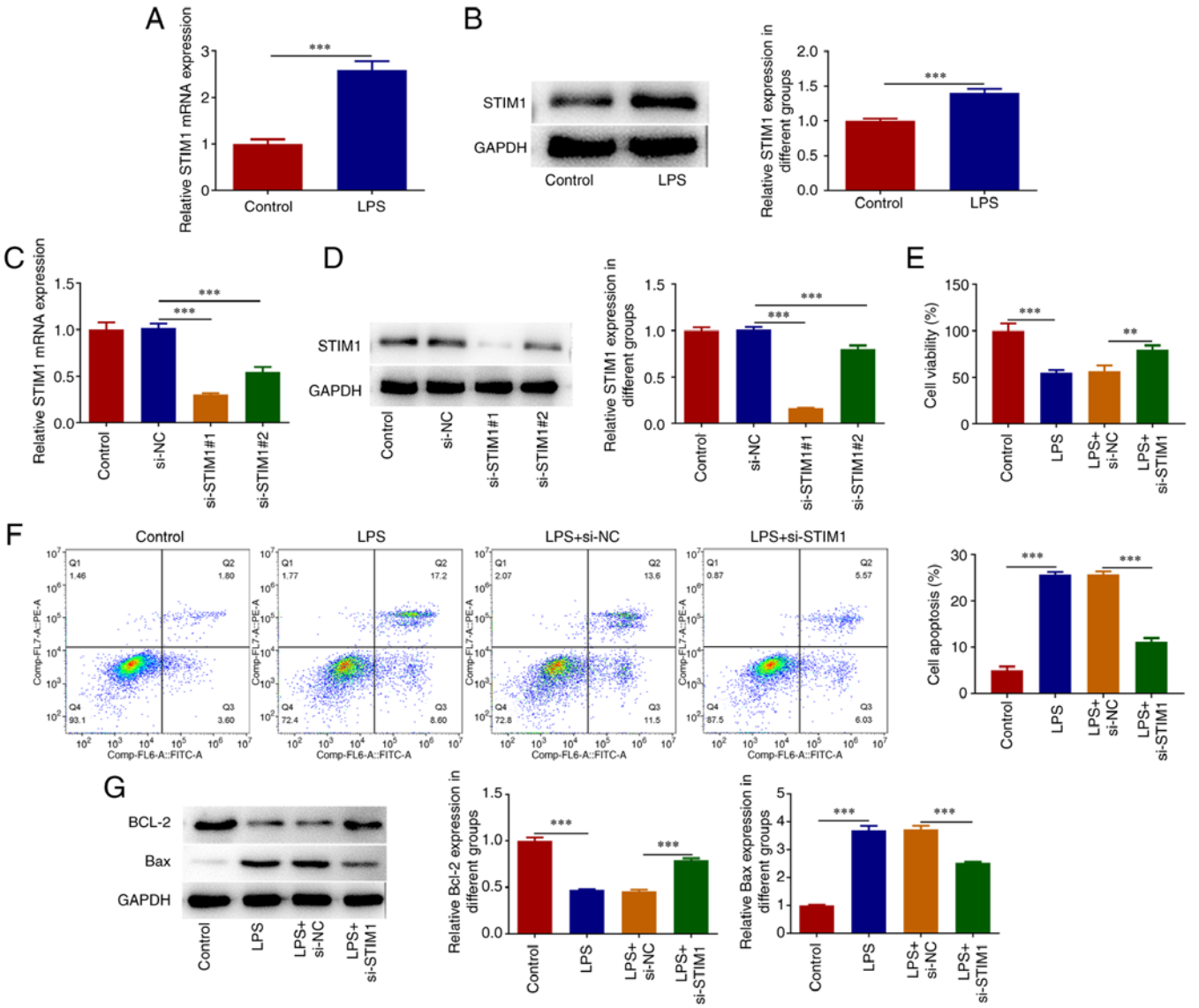

Figure 1. *STIM1* expression is increased in LPS-induced A549 cells and *STIM1* knockdown inhibits LPS-induced A549 cell apoptosis. The expression of *STIM1* was detected by (A) RT-qPCR and (B) western blotting. The *STIM1* interference plasmid was constructed and transfected into A549 cells and the transfection efficacy was detected by (C) RT-qPCR and (D) western blotting. (E) Cell viability was assessed by Cell Counting Kit-8. (F) Flow cytometry was used to detect cell apoptosis. (G) Western blotting was used to detect apoptosis-related proteins. **P<0.01 and ***P<0.001. *STIM1*, stromal interaction molecule 1; LPS, lipopolysaccharide; NC, negative control; RT-qPCR, reverse transcription-quantitative PCR; si, small interfering (RNA).

down by anti-IGF2BP2 in cells (Fig. 3C). *IGF2BP2* interference and overexpression plasmids were constructed and transfected into A549 cells and the transfection efficacy was detected by RT-qPCR and western blotting (Fig. 3D and E). Following this, si-*IGF2BP2*#1 was chosen for the follow-up experiments. After actinomycin D treatment, the stability of *STIM1* mRNA decreased upon *IGF2BP2* inhibition (Fig. 3F). Next, cells were divided into the control, si-NC, si-*IGF2BP2*, Oe-NC and Oe-*IGF2BP2* groups and the *STIM1* expression level in these groups was detected by RT-qPCR and western blotting. The results demonstrated that the expression of *STIM1* decreased significantly after *IGF2BP2* expression was inhibited. Furthermore, overexpression of *IGF2BP2* significantly increased the expression of *STIM1* in cells (Fig. 3G and H). Next, cells were divided into the control, LPS, LPS + si-*STIM1*, LPS + si-*STIM1* + Oe-NC and LPS + si-*STIM1* + Oe-*IGF2BP2* groups. RT-qPCR results showed that *STIM1* expression was significantly inhibited in LPS + si-*STIM1* group compared with LPS group. Compared with LPS + si-*STIM1* + Oe-NC group, the expression of *STIM1* was increased in LPS + si-*STIM1* + Oe-*IGF2BP2* group (Fig. 3I).

Knockdown of IGF2BP2-regulated STIM1 expression alleviates LPS-induced ERS and inflammatory responses in A549 cells. The results demonstrated that overexpression of *IGF2BP2* reversed the inhibitory effect of *STIM1* knockdown on the LPS-induced apoptosis of A549 cells (Fig. 4A-C). The ELISA results demonstrated that, compared with the LPS + si-*STIM1* + Oe-NC group, the levels of IL-1β and TNF-α in the LPS + si-*STIM1* + Oe-*IGF2BP2* group were significantly increased, IL-6 showed an increasing trend, but it was not marked (Fig. 4D). Furthermore, the results of the IF assay showed that overexpression of *IGF2BP2*

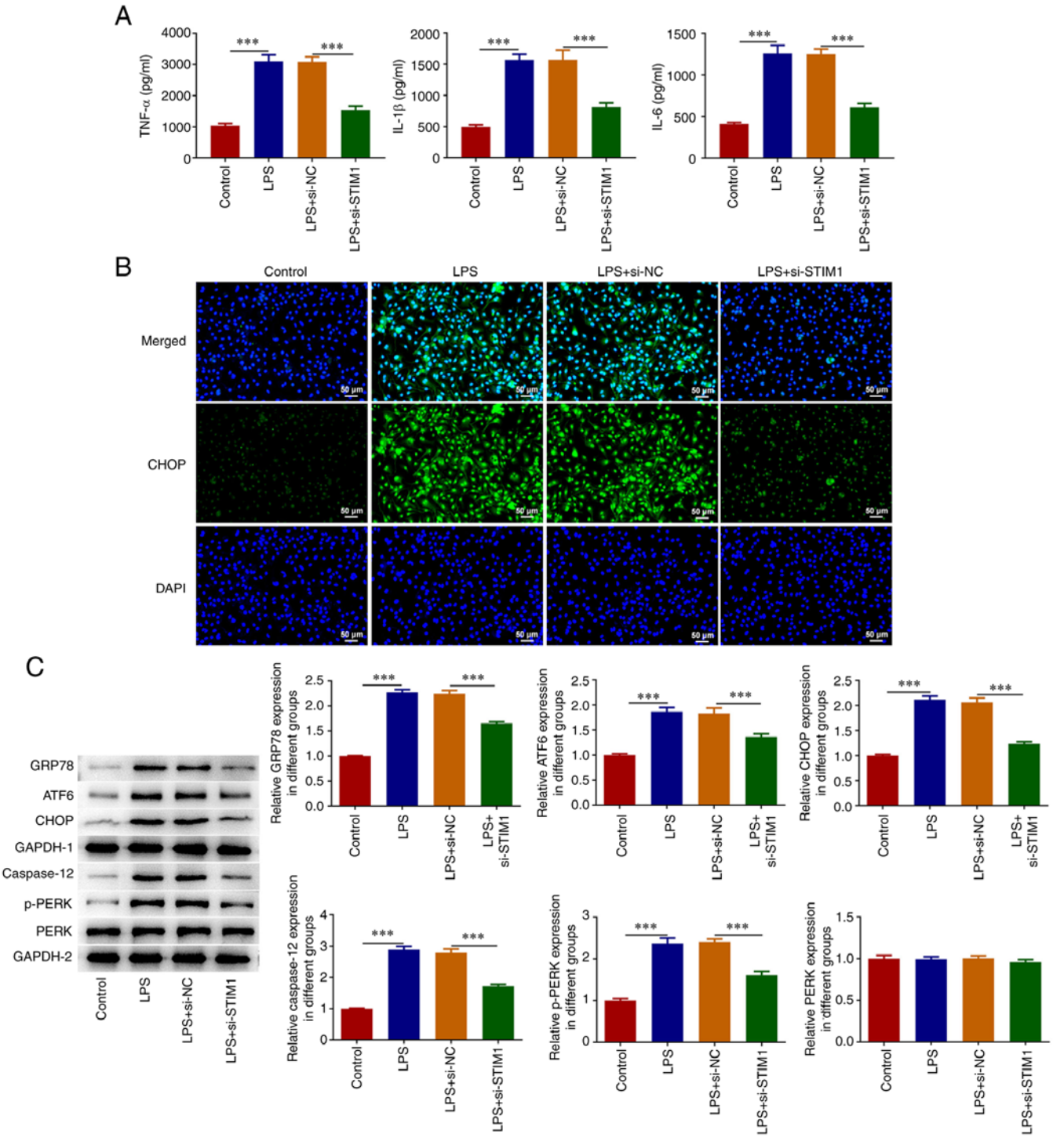

Figure 2. *STIM1* knockdown alleviates LPS-induced A549 cell inflammation and ER stress. (A) Enzyme-linked immunosorbent assay kits were used to detect the levels of inflammatory cytokines. (B) Immunofluorescence assay was used to detect the expression of CHOP. (C) Western blotting was used to detect the expression of GRP78, ATF6, CHOP, caspase 12 and p-PERK. ***P<0.001. *STIM1*, stromal interaction molecule 1; LPS, lipopolysaccharide; ATF6, activating transcription factor 6; ER, endoplasmic reticulum; CHOP, C/EBP homologous protein; GRP78, glucose-regulated protein 78; NC, negative control; p-PERK, phosphorylated PKR-like ER kinase; si, small interfering RNA.

reversed the inhibitory effect of *STIM1* knockdown on CHOP expression in LPS-induced A549 cells (Fig. 5A). In addition, western blotting analysis demonstrated that, compared with the LPS + si-*STIM1* + Oe-NC group, the levels of GRP78, ATF6, CHOP, caspase 12 and p-PERK in the LPS + si-*STIM1* + Oe-NC group were significantly increased (Fig. 5B).

Discussion

Pneumonia is a severe infectious disease attributed to a number of pathogenic factors, among which bacterial pneumonia is the most common. LPS, a major component of the gram-negative bacterial cell wall, is a common inducer of the inflammatory response in tissues and cells (26,27). After gram-negative bacteria enters the

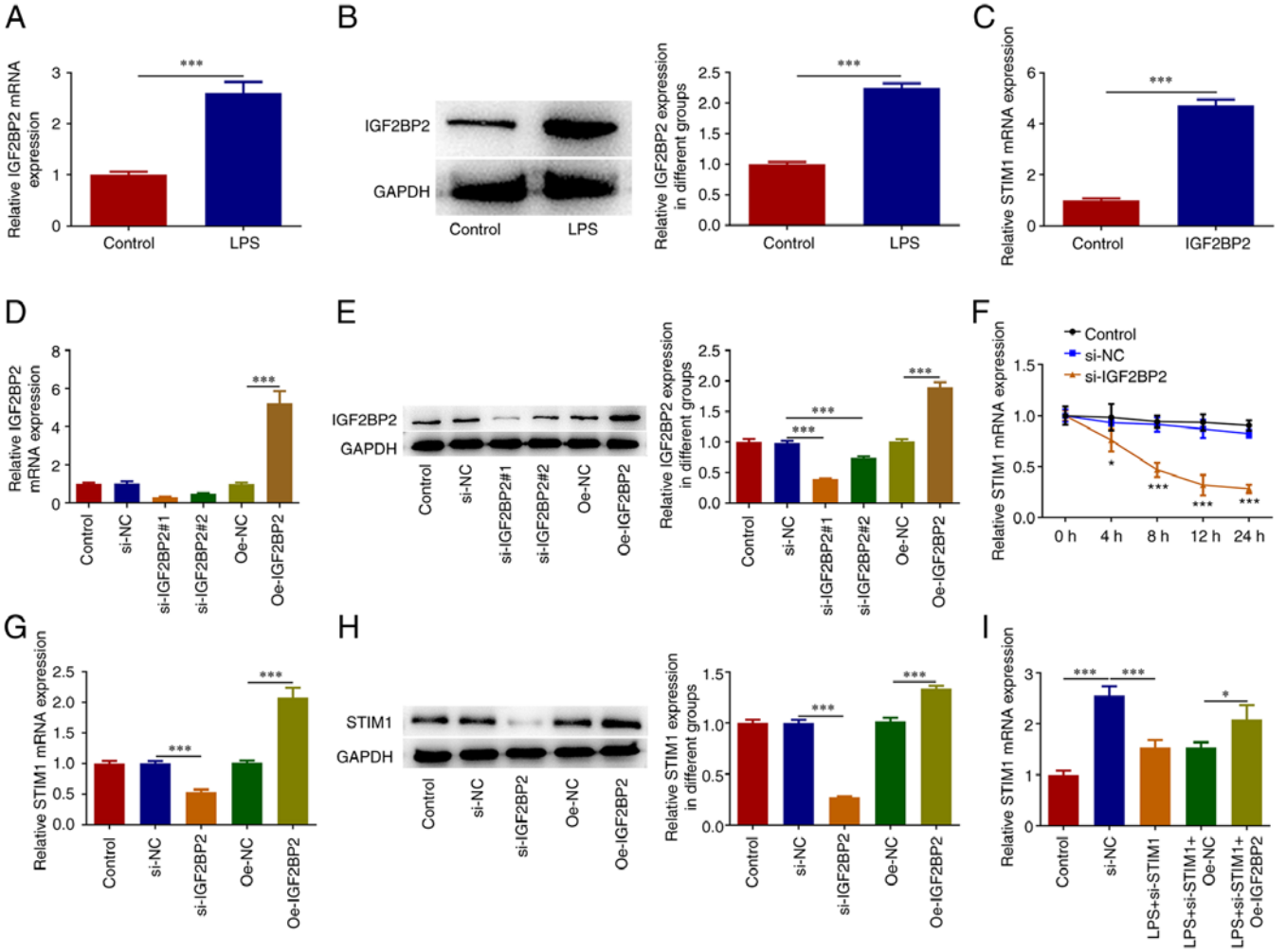

Figure 3. *IGF2BP2* enhances the stability of *STIM1* mRNA. The expression of *IGF2BP2* was detected by (A) RT-qPCR and (B) western blotting. (C) *STIM1* mRNA levels were measured in RNA pulled down by anti-*IGF2BP2* in cells. *IGF2BP2* interference and overexpression plasmids were constructed and transfected into A549 cells and the transfection efficacy was detected by (D) RT-qPCR and (E) western blotting. (F) After actinomycin D treatment, the stability of *STIM1* mRNA was detected by RT-qPCR. The *STIM1* expression level was detected by (G) RT-qPCR and (H) western blotting. (I) The *STIM1* expression level was detected by RT-qPCR after inhibiting STIM1 and overexpressing IGF2BP2 simultaneously. *P<0.05, ***P<0.001. *IGF2BP2*, insulin-like growth factor 2 mRNA binding protein 2; *STIM1*, stromal interaction molecule 1; RT-qPCR, reverse transcription-quantitative PCR; LPS, lipopolysaccharide; NC, negative control; Oe, overexpression; si, small interfering RNA.

body, LPS can induce chemotaxis, migration and eventually infiltration of the lung tissues and, accompanied by the upregulation of inflammatory mediators, ultimately lead to the occurrence of acute lung injury (28). Hence, LPS is often used as an inducer for acute lung injury models. In the present study, LPS was used to construct a lung injury model using A549 cells. The results demonstrated that LPS led to significantly decreased cell viability and increased apoptosis and inflammatory response, which indicated the successful construction of the model.

Classical ERS receptors are ER membrane proteins, PERK and ATF6. Typically, when these receptor proteins are bound to the GRP78 molecular chaperone, they are inactive and become activated upon dissociation from GRP78 during ERS, triggering downstream events through signal transduction (29). In addition, upregulation of CHOP transcription factor may induce the inflammatory response and apoptosis and promote the occurrence and development of diseases (30,31). Inhibition of ERS-mediated apoptosis has been reported to reduce susceptibility to *Streptococcus pneumoniae* co-infection after influenza infection (32). Furthermore, ginsenoside Rg1 regulates sirtuin 1 and improves lung inflammation and injury caused by sepsis by inhibiting ERS and inflammation (33). In addition, caspase12 is a pro-apoptotic molecule specific to the outer membrane of the ER and activation of caspase12 is one of the core links in the development of ERS phase decay (34). In the present study, LPS was administered to A549 cells to induce ERS injury. The expression of ERS-related proteins, GRP78, ATF6, CHOP, caspase 12 and p-PERK, were significantly increased after LPS induction. These results indicated that LPS induced ERS injury in A549 cells.

In the present study, it was found that *STIM1* expression was significantly elevated in LPS-induced A549 cells. *STIM1* is a newly discovered human gene located in a specific region of human chromosome 11p15.5 (35). *STIM1* is involved in the regulation of the inflammatory processes. Regulation of *STIM1*/*Orai1* signaling in bovine mammary epithelial cells has been shown to alleviate LPS-induced inflammation (17). In addition, the expression of *STIM1* and Orai1 is upregulated when exposed to a high water volume or large cyclic stretching, which further activates calcium-sensitive protein kinase Cα, leading to calcium overload, excessive endothelial permeability

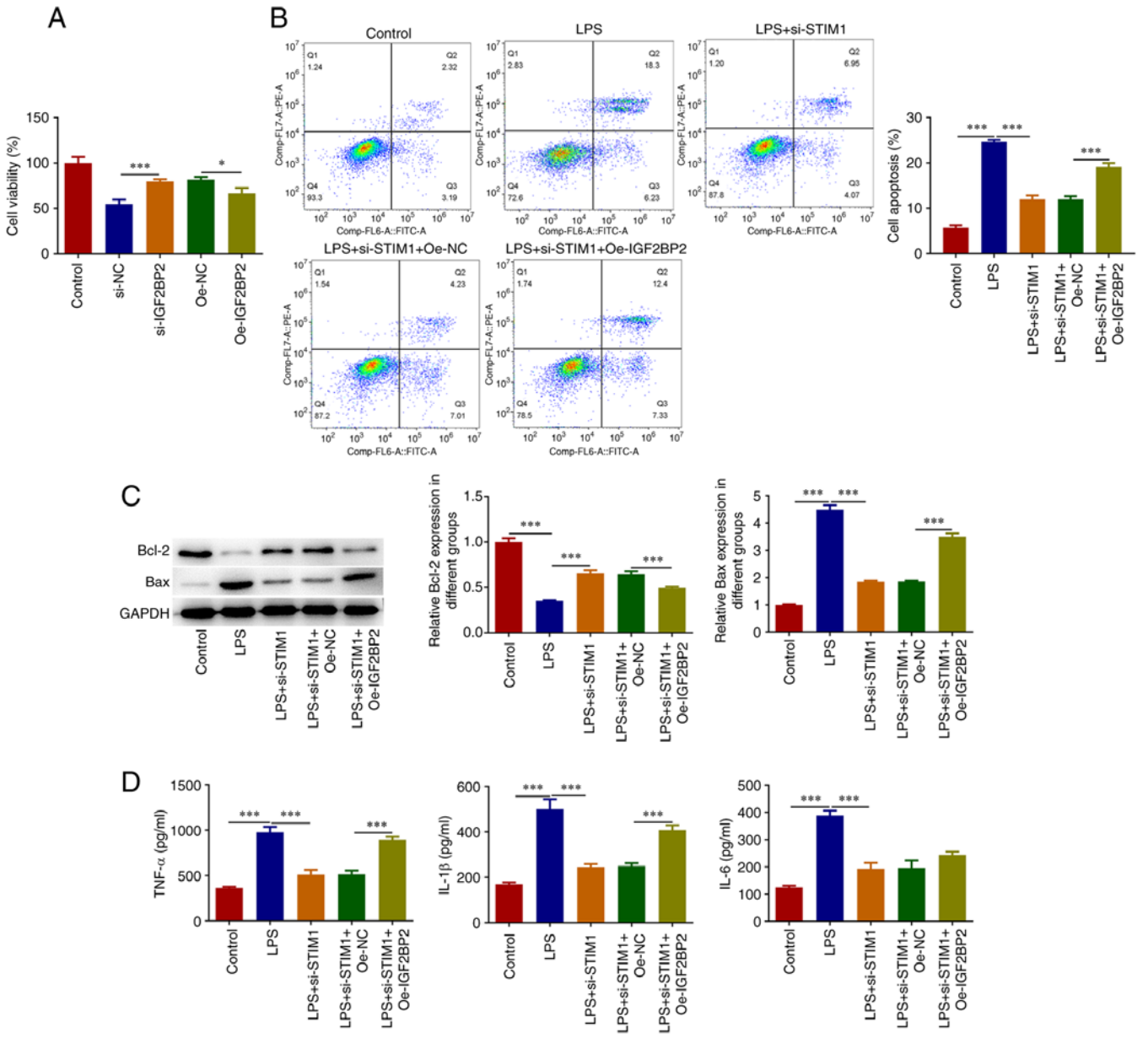

Figure 4. Knockdown of *IGF2BP2*-regulated *STIM1* expression alleviates LPS-induced inflammatory responses in A549 cells. (A) Cell viability was assessed by Cell Counting Kit-8. (B) Flow cytometry was used to detect cell apoptosis. (C) Western blotting was used to detect apoptosis-related proteins. (D) Enzyme-linked immunosorbent assay kits were used to detect the levels of inflammatory cytokines. *P<0.05 and ***P<0.001. *IGF2BP2*, insulin-like growth factor 2 mRNA binding protein 2; *STIM1*, stromal interaction molecule 1; LPS, lipopolysaccharide; NC, negative control; Oe, overexpression; si, small interfering RNA.

and ultimately ventilator-induced lung injury (36). *STIM1* activation also mediates S-phase stagnation and cell death in acute pulmonary poisoning induced by paraquat (37). In addition, *STIM1*-Orai1 interaction exacerbates LPS-induced bovine hepatocyte inflammation and ERS through store-operated calcium entry (9). However, to the best of the authors' knowledge, the role of *STIM1* in LPS-induced A549 cell injury has not yet been reported. In the present study, it was found that inhibition of *STIM1* expression in LPS-induced A549 cells significantly inhibited LPS-induced apoptosis, inflammation and ERS.

In the present study, through RIP and other experiments, it was demonstrated that IGF2BP2 could enhance the stability of *STIM1* mRNA. A previous study demonstrated that *IGF2BP2* knockdown inhibited LPS-induced inflammation of lung epithelial cells by targeting caspase 4, thus inhibiting the non-standard scorching pathway (19). In addition, ameliorating TGF-β-activated kinase 1 binding protein 3 N^6-methyladenine modification by *IGF2BP2*-dependent mechanisms reduces kidney injury and inflammation (38). In the present study, it was found that overexpression of *IGF2BP2* reversed the inhibitory effect of *STIM1* knockdown on LPS-induced apoptosis, inflammation and ERS in A549 cells.

The present study also has certain limitations. First, it only investigated IGF2BP2-dependent *STIM1* inhibition in cells and did not verify it in animals. The conclusions will be verified in animals in future experiments. Second, the present study showed that the abnormality of IGF2BP2 can affect the immune response of the body (39). Will the subsequent downregulation of *IGF2BP2* indirectly affect the expression of *STIM1*, rather than because of the influence on *STIM1*? This will be explored further in future experiments. In addition, as for the experiments

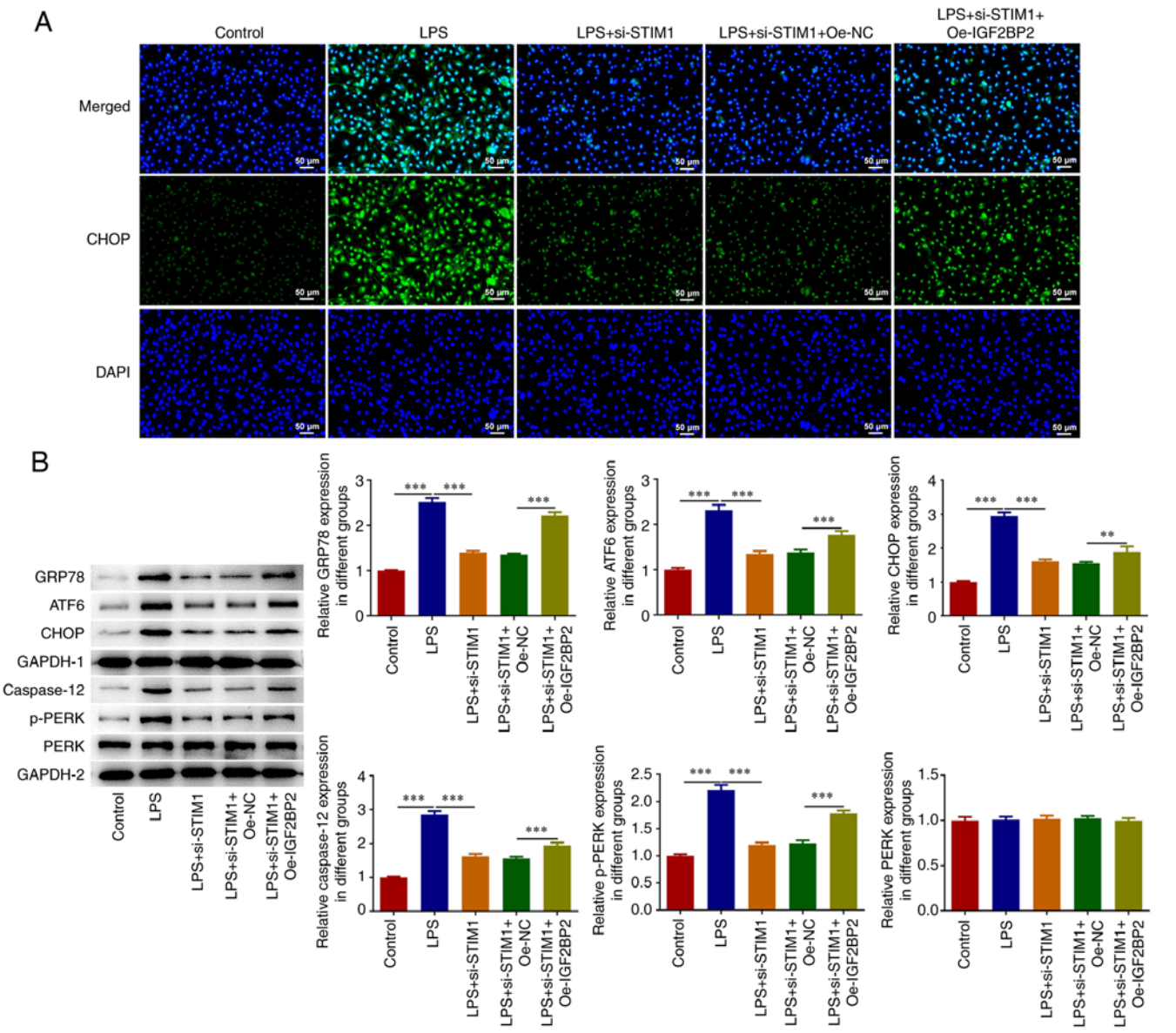

Figure 5. Knockdown of *IGF2BP2*-regulated *STIM1* expression alleviates LPS-induced ER stress in A549 cells. (A) An immunofluorescence assay was used to detect the expression of CHOP. (B) Western blotting was used to detect the expression of GRP78, ATF6, CHOP, caspase 12 and p-PERK. **P<0.01, ***P<0.001. *IGF2BP2*, insulin-like growth factor 2 mRNA binding protein 2; *STIM1*, stromal interaction molecule 1; LPS, lipopolysaccharide; ER, endoplasmic reticulum; CHOP, C/EBP homologous protein; GRP78, glucose-regulated protein 78; ATF6, activating transcription factor 6; NC, negative control; Oe, overexpression; p-PERK, phosphorylated PKR-like ER kinase; si, small interfering (RNA).

for *STIM1* overexpression, it is still necessary to further verify the experiment and this will be discussed in future studies.

In conclusion, knockdown of IGF2BP2-regulated STIM1 expression protects against LPS-induced pneumonia *in vitro* by alleviating ERS and the inflammatory response.

Acknowledgements

Not applicable.

Funding

The present study was supported by National K&D Program of China (grant no. 2022YFC2304800), Guangzhou Medical Key Discipline (grant no. 2021-2023) and Guangzhou Science and Technology Planning Project (grant no. 2023A03J0534).

Availability of data and materials

The data sets analyzed and/or generated during the present study are available from the corresponding author on reasonable request.

Authors' contributions

JH conceived the present study. WZ, QD, NS and ZL performed the experiments. WZ wrote the manuscript. QD, NS and ZL processed the experimental data and JH ensured the accuracy of the experimental data. WZ and JH confirm the authenticity of all the raw data. All authors read and approved the final manuscript.

Ethics approval and consent to participate

Not applicable.

Patient consent for publication

Not applicable.

Competing interests

The authors declare that they have no competing interests.

References

1. Bordon J, Aliberti S, Fernandez-Botran R, Uriarte SM, Rane MJ, Duvvuri P, Peyrani P, Morlacchi LC, Blasi F and Ramirez JA: Understanding the roles of cytokines and neutrophil activity and neutrophil apoptosis in the protective versus deleterious inflammatory response in pneumonia. Int J Infect Dis 17: e76-83, 2013.
2. Hespanhol V and Barbara C: Pneumonia mortality, comorbidities matter? Pulmonology 26: 123-129, 2020.
3. Bartoletti M, Azap O, Barac A, Bussini L, Ergonul O, Krause R, Paño-Pardo JR, Power NR, Sibani M, Szabo BG, *et al*: ESCMID COVID-19 living guidelines: Drug treatment and clinical management. Clin Microbiol Infect 28: 222-238, 2022.
4. Torres A, Cilloniz C, Niederman MS, Menendez R, Chalmers JD, Wunderink RG and van der Poll T: Pneumonia. Nat Rev Dis Primers 7: 25, 2021.
5. Prina E, Ranzani OT and Torres A: Community-acquired pneumonia. Lancet 386: 1097-1108, 2015.
6. Khan MM, Yang WL and Wang P: Endoplasmic reticulum stress in sepsis. Shock 44: 294-304, 2015.
7. Liu Q, Korner H, Wu H and Wei W: Endoplasmic reticulum stress in autoimmune diseases. Immunobiology 225: 151881, 2020.
8. Cao X, Wan H and Wan H: Urolithin A induces protective autophagy to alleviate inflammation, oxidative stress and endoplasmic reticulum stress in pediatric pneumonia. Allergol Immunopathol (Madr) 50: 147-153, 2022.
9. Xue Y, Zhou S, Xie W, Meng M, Ma N, Zhang H, Wang Y, Chang G and Shen X: STIM1-Orai1 interaction exacerbates LPS-induced inflammation and endoplasmic reticulum stress in bovine hepatocytes through store-operated calcium entry. Genes (Basel) 13: 874, 2022.
10. Li Y, Feng YF, Liu XT, Li YC, Zhu HM, Sun MR, Li P, Liu B and Yang H: Songorine promotes cardiac mitochondrial biogenesis via Nrf2 induction during sepsis. Redox Biol 38: 101771, 2021.
11. Pan S, Zhao X, Shao C, Fu B, Huang Y, Zhang N, Dou X, Zhang Z, Qiu Y, Wang R, *et al*: STIM1 promotes angiogenesis by reducing exosomal miR-145 in breast cancer MDA-MB-231 cells. Cell Death Dis 12: 38, 2021.
12. Garrud TAC and Jaggar JH: STIMulating blood pressure. Elife 11: e77978, 2022.
13. Bolotina VM: Orai1, STIM1, and iPLA2beta determine arterial vasoconstriction. Arterioscler Thromb Vasc Biol 32: 1066-1067, 2012.
14. Li H, Jiang Z, Liu X and Yang Z: Higher plasma level of STIM1, OPG are correlated with stent restenosis after PCI. Int J Clin Exp Med 8: 21089-21097, 2015.
15. Zhu X, Huang H, Zong Y and Zhang L: SRY-related high-mobility group box 9 (SOX9) alleviates cigarette smoke extract (CSE)-induced inflammatory injury in human bronchial epithelial cells by suppressing stromal interaction molecule 1 (STIM1) expression. Inflamm Res 71: 565-576, 2022.
16. Liu CC, Miao Y, Chen RL, Zhang YQ, Wu H, Yang SM and Shang LQ: STIM1 mediates IAV-induced inflammation of lung epithelial cells by regulating NLRP3 and inflammasome activation via targeting miR-223. Life Sci 266: 118845, 2021.
17. Meng M, Huo R, Ma N, Chang G and Shen X: beta-carotene alleviates LPS-induced inflammation through regulating STIM1/ORAI1 expression in bovine mammary epithelial cells. Int Immunopharmacol 113: 109377, 2022.
18. Xu X, Shen HR, Zhang JR and Li XL: The role of insulin-like growth factor 2 mRNA binding proteins in female reproductive pathophysiology. Reprod Biol Endocrinol 20: 89, 2022.
19. Wang J, Yuan X and Ding N: IGF2BP2 knockdown inhibits LPS-induced pyroptosis in BEAS-2B cells by targeting caspase 4, a crucial molecule of the non-canonical pyroptosis pathway. Exp Ther Med 21: 593, 2021.
20. Paz I, Kosti I, Ares M Jr, Cline M and Mandel-Gutfreund Y: RBPmap: A web server for mapping binding sites of RNA-binding proteins. Nucleic Acids Res 42: W361-W367, 2014.
21. Chen W, Xu S, Xiang L, Zhang Y, Wang C, Fan T, Huang W and Lu Z: The silencing of SAAL1 suppresses pneumonia progression via modulating the NLR signaling pathway. Ann Transl Med 10: 1128, 2022.
22. Fei S, Cao L and Pan L: microRNA-3941 targets IGF2 to control LPS-induced acute pneumonia in A549 cells. Mol Med Rep 17: 4019-4026, 2018.
23. Shi J, Wang H, Liu J, Zhang Y, Luo J, Li Y, Yang C and Jiang J: Ganoderic acid B attenuates LPS-induced lung injury. Int Immunopharmacol 88: 106990, 2020.
24. Livak KJ and Schmittgen TD: Analysis of relative gene expression data using real-time quantitative PCR and the 2(-Delta Delta C(T)) method. Methods 25: 402-408, 2001.
25. Wu H, Xu J, Gong G, Zhang Y and Wu S: CircARL8B contributes to the development of breast cancer via regulating miR-653-5p/HMGA2 axis. Biochem Genet 59: 1648-1665, 2021.
26. Yang R, Liu H, Bai C, Wang Y, Zhang X, Guo R, Wu S, Wang J, Leung E, Chang H, *et al*: Chemical composition and pharmacological mechanism of Qingfei Paidu Decoction and Ma Xing Shi Gan Decoction against Coronavirus Disease 2019 (COVID-19): In silico and experimental study. Pharmacol Res 157: 104820, 2020.
27. Gao P, Wang J, Jiang M, Li Z, Xu D, Jing J, Yihepaer and Hu T: LncRNA SNHG16 is downregulated in Pneumonia and Downregulates miR-210 to promote LPS-induced lung cell apoptosis. Mol Biotechnol 65: 446-452, 2023.
28. Zhang Y, Zhu Y, Gao G and Zhou Z: Knockdown XIST alleviates LPS-induced WI-38 cell apoptosis and inflammation injury via targeting miR-370-3p/TLR4 in acute pneumonia. Cell Biochem Funct 37: 348-358, 2019.
29. Yang YF, Wang H, Song N, Jiang YH, Zhang J, Meng XW, Feng XM, Liu H, Peng K and Ji FH: Dexmedetomidine Attenuates Ischemia/Reperfusion-Induced Myocardial inflammation and apoptosis through inhibiting endoplasmic reticulum stress Signaling. J Inflamm Res 14: 1217-1233, 2021.
30. Keestra-Gounder AM, Byndloss MX, Seyffert N, Young BM, Chavez-Arroyo A, Tsai AY, Cevallos SA, Winter MG, Pham OH, Tiffany CR, *et al*: NOD1 and NOD2 signalling links ER stress with inflammation. Nature 532: 394-397, 2016.
31. Kim I, Xu W and Reed JC: Cell death and endoplasmic reticulum stress: Disease relevance and therapeutic opportunities. Nat Rev Drug Discov 7: 1013-1030, 2008.
32. Wang X, Yuan J, Wang H, Gan N, Zhang Q, Liu B, Wang J, Shu Z, Rao L, Gou X, *et al*: Progranulin decreases susceptibility to streptococcus pneumoniae in influenza and protects against lethal coinfection. J Immunol 203: 2171-2182, 2019.
33. Wang QL, Yang L, Peng Y, Gao M, Yang MS, Xing W and Xiao XZ: Ginsenoside Rg1 regulates SIRT1 to ameliorate sepsis-induced lung inflammation and injury via inhibiting endoplasmic reticulum stress and inflammation. Mediators Inflamm 2019: 6453296, 2019.
34. Wu JP, Li XZ, Wang Y, Ma L, Yao TW, Zhang YY and Long F: Effects of electroacupuncture and intracerebral injection of VEGF on Caspase12, Caspase3, and GRP78 genes in rats with cerebral ischemia-reperfusion injury. Sichuan Da Xue Xue Bao Yi Xue Ban 50: 34-39, 2019 (In Chinese).
35. Parker NJ, Begley CG, Smith PJ and Fox RM: Molecular cloning of a novel human gene (D11S4896E) at chromosomal region 11p15.5. Genomics 37: 253-256, 1996.
36. Song X, Liu Y, Dong L and Wang Y: Stromal-Interacting Molecule 1 (Stim1)/Orai1 modulates endothelial permeability in ventilator-induced lung injury. Med Sci Monit 24: 9413-9423, 2018.
37. Fan H, Huang H, Hu L, Zhu W, Yu Y, Lou J, Hu L and Chen F: The activation of STIM1 mediates S-phase arrest and cell death in paraquat induced acute lung intoxication. Toxicol Lett 292: 123-135, 2018.
38. Wang JN, Wang F, Ke J, Li Z, Xu CH, Yang Q, Chen X, He XY, He Y, Suo XG, *et al*: Inhibition of METTL3 attenuates renal injury and inflammation by alleviating TAB3 m6A modifications via IGF2BP2-dependent mechanisms. Sci Transl Med 14: eabk2709, 2022.
39. Zhou L, Li H, Cai H, Liu W, Pan E, Yu D and He S: Upregulation of IGF2BP2 promotes oral squamous cell carcinoma progression that is related to cell proliferation, metastasis and tumor-infiltrating immune cells. Front Oncol 12: 809589, 2022.